

Design and Characterization of Immobilized Enzymes in Microfluidic Systems

Hanbin Mao, Tinglu Yang, and Paul S. Cremer*

Department of Chemistry, Texas A&M University, P.O. Box 30012, College Station, Texas 77842-3012

Herein we report the fabrication, characterization, and use of total analytical microsystems containing surface-immobilized enzymes. Streptavidin-conjugated alkaline phosphatase was linked to biotinylated phospholipid bilayers coated inside poly(dimethylsiloxane) microchannels and borosilicate microcapillary tubes. Rapid determination of enzyme kinetics at many different substrate concentrations was made possible by carrying out laminar flow-controlled dilution on-chip. This allowed Lineweaver–Burk analysis to be performed from a single experiment with all the data collected simultaneously. The results revealed an enzyme turnover number of $51.1 \pm 3.2 \text{ s}^{-1}$ for this heterogeneous system. Furthermore, the same enzyme immobilization strategy was extended to demonstrate that multiple chemical reactions could be performed in sequence by immobilizing various enzymes in series. Specifically, the presence of glucose was detected by two coupled steps employing immobilized avidinD-conjugated glucose oxidase and streptavidin-conjugated horseradish peroxidase.

Microfluidic devices have gained a great deal of attention over the last several years due to their potential for creating inexpensive analytical tools with minute volumes and high throughput as well as for their potential for mass replication.¹ A host of diagnostic applications can be coupled to these systems for immunoassay development,^{2,3} biosensor design,^{4,5} genetics,^{6–8} and cell screening.⁹ Furthermore, microfluidics can be exploited for patterning surfaces with biological materials at micrometer-scale resolution. There have been several reports dealing with patterning proteins,¹⁰ cells,¹¹ and planar lipid bilayers.¹²

Several investigators have also begun to explore the role that enzymes could play in microfluidics for developing lab-on-a-chip technologies. For example, Duffy and co-workers developed a centrifugal microfluidic system capable of measuring dozens of enzymatic assays simultaneously in a homogeneous format.¹³ They exploited this apparatus to measure a substrate inhibition constant for binding to an enzyme in a single experiment. In another homogeneous assay, Hadd and co-workers employed computer-controlled electrokinetic transport for analysis and electrophoretic separation of enzyme inhibitors.⁴ Extending such work to heterogeneous assays with immobilized enzymes would provide distinct advantages over homogeneous formats for applications such as chemical synthesis and assay reuse because reactants can flow in and products flow out without disrupting the catalysts. Indeed, a few groups have already begun exploring procedures for immobilizing enzymes in microfluidic devices for use in heterogeneous assays. Examples include work by Kim and co-workers, which showed that enzymes could be imbedded inside sol–gel structures.¹⁴ Another example is the work of Eteshola and Leckband that undertook the design of an ELISA assay inside PDMS microfluidic channels.¹⁵

In the studies presented here, we developed a simple method for immobilizing biocatalysts on the walls of PDMS microfluidic channels for three specific goals. First, we wanted to find a simple strategy for protein immobilization within lab-on-a-chip devices for use in rapid prototyping experiments. In particular, we wanted to do this for PDMS molds bonded to glass as this system is in wide use. The challenge for such work, however, lay in the fact that immobilization methods needed to be developed such that both the PDMS and glass surfaces accommodated protein attachment while still preserving reasonable enzymatic activity. Second, we wanted to exploit such methods for obtaining enzyme turnover rates and related kinetic data in a massively parallel fashion with good signal-to-noise properties. Finally, we wanted to test the feasibility of employing such methods for the immobilization of several different catalysts in a series for use in multistep or coupled chemical reactions.

* To whom correspondence should be addressed: (tel) (979) 862-1200; (fax) (979) 845-7561, (e-mail) cremer@mail.chem.tamu.edu.

- (1) Figeys, D.; Pinto, D. *Anal. Chem.* **2000**, *72*, 330A–335A.
- (2) Chiem, N.; Harrison, D. J. *Anal. Chem.* **1997**, *69*, 373–378.
- (3) Chiem, N. H.; Harrison, D. J. *Electrophoresis* **1998**, *19*, 3040–3044.
- (4) Hadd, A. G.; Jacobson, S. C.; Ramsey, J. M. *Anal. Chem.* **1999**, *71*, 5206–5212.
- (5) Santini, J. T.; C., R. A.; Scheidt, R.; Cima, M. J.; Langer, R. *Angew. Chem., Int. Ed.* **2000**, *39*, 2397–2407.
- (6) Khandurina, J.; McKnight, T. E.; Jacobson, S. C.; Waters, L. C.; Foote, R. S.; Ramsey, J. M. *Anal. Chem.* **2000**, *72*, 2995–3000.
- (7) Burns, M. A.; Johnson, B. N.; Brahmasandra, S. N.; Handique, K.; Webster, J. R.; Krishnan, M.; Sammarco, T. S.; Man, P. M.; Jones, D.; Heldsinger, D.; Mastrangelo, C. H.; Burke, D. T. *Science* **1998**, *282*, 484–487.
- (8) Lagally, E. T.; Simpson, P. C.; A., M. R. *Sens. Actuators, B* **2000**, *63*, 138–146.
- (9) Sohn, L. L.; Saleh, O. A.; Facer, G. R.; Beavis, A. J.; Allan, R. S.; Notterman, D. A. *Proc. Natl. Acad. Sci. U.S.A.* **2000**, *97*, 10687–10690.
- (10) Delamarche, E.; Bernard, A.; Schmid, H.; Michel, B.; Biebuyck, H. *Science* **1997**, *276*, 779–781.
- (11) Chiu, D. T.; Jeon, N. L.; Huang, S.; Kane, R. S.; Wargo, C. J.; Choi, I. S.; Ingber, D. E.; Whitesides, G. M. *Proc. Natl. Acad. Sci. U.S.A.* **2000**, *97*, 2408–2413.
- (12) Yang, T.; Jung, S. Y.; Mao, H.; Cremer, P. S. *Anal. Chem.* **2001**, *73*, 165–169.
- (13) Duffy, D. C.; Gillis, H. L.; Lin, J.; Sheppard, N. F. J.; Kellogg, G. J. *Anal. Chem.* **1999**, *71*, 4669–4678.
- (14) Kim, Y.; Park, C. B.; Clark, D. S. *Biotechnol. Bioeng.* **2001**, *73*, 331–337.
- (15) Eteshola, E.; Leckband, D. *Sens. Actuators, B* **2001**, *72*, 129–133.

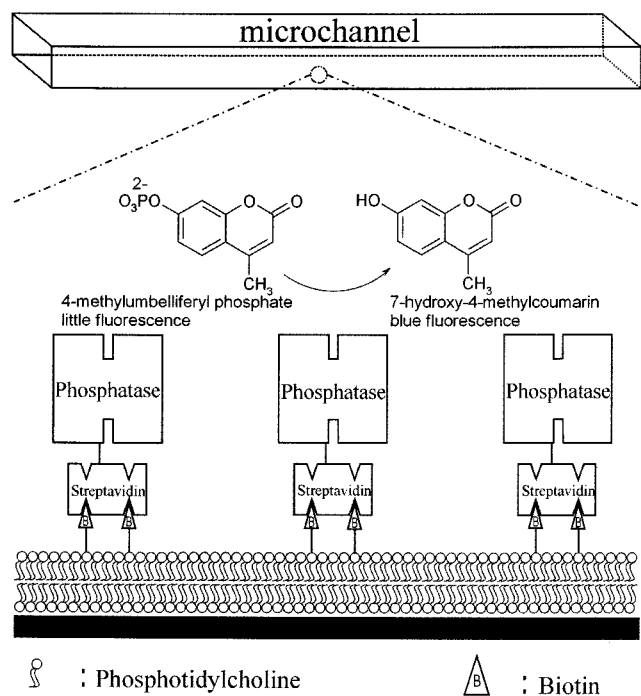


Figure 1. Schematic diagram of streptavidin-conjugated alkaline phosphatase bound to a supported lipid bilayer containing biotinylated lipids. The deciivities in the enzyme represent its two active sites, while the four deciivities in the streptavidin represent its four biotin binding sites.

The strategy adopted for this work was to employ biotin–streptavidin chemistry in conjunction with supported phospholipid membranes for surface immobilization of the enzymes^{16–18} (Figure 1). We have previously shown that lipid bilayers containing specific recognition elements can be completely coated on the inside of PDMS microfluidic channels bound to glass supports.¹² The bilayer coating is formed by the fusion of small unilamellar vesicles (SUVs) to the surfaces of both the glass and PDMS, if the latter is rendered hydrophilic. When a small percentage of the lipid headgroups is biotinylated, an enzyme of interest can be bound to the surface, if it is in turn linked to streptavidin. In this case, the lipid bilayer serves as a buffer to prevent the protein from denaturing on the underlying surface and could, under proper circumstances, provide a method for obtaining uniform orientation. Indeed, this method has been shown to be a viable means of maintaining a high degree of protein structure and orientation in corresponding planar systems.^{17,18} Furthermore, because the bilayer is two-dimensionally fluid, enzymes can reorganize at the interface to achieve high packing densities. It may also be possible to modify bilayer-based assays to accommodate membrane proteins.

This paper is laid out in the following manner. In the first section, we immobilized phosphatase enzymes inside glass microcapillary tubes containing no PDMS. The turnover rate of the catalysts were measured and compared with results in the second section for enzymes inside an array of PDMS microchannels. The results indicated that the turnover rate for dephosphorylation was

the same for both systems within experimental error. Furthermore, the use of the PDMS system made data collection more than 1 order of magnitude more rapid than in the microcapillary platform, while possessing an improved signal-to-noise ratio. In the final section of this work, we immobilized glucose oxidase and horseradish peroxidase in series to create a simple glucose sensor that works in two steps.

EXPERIMENTAL SECTION

Materials. Phospholipid vesicles were formed from 1,2-dilauroyl-*sn*-glycero-3-phosphocholine (DLPC), 1,2-dipalmitoyl-*sn*-glycero-3-phosphoethanolamine-*N*-(7-nitro-2-1,3-benzoxadiazol-4-yl) (NBD-Cap-PE), and N-Biotinyl-Cap-PE (16:0) (Avanti Polar Lipids, Inc, Alabaster, AL). Texas Red-labeled streptavidin, streptavidin-conjugated alkaline phosphatase (1:1 stoichiometry), streptavidin-conjugated horseradish peroxidase (1:1 stoichiometry), Amplex Red, and 4-methylumbelliferyl phosphate were purchased from Molecular Probes (Eugene, OR). This particular phosphate derivative was chosen because dephosphorylation generates the highly fluorescent soluble product, 7-hydroxy-4-methylcoumarin. AvidinD-conjugated glucose oxidase (1:1 stoichiometry, 0.5 mg/mL) was purchased from Vector Laboratories (Burlingame, CA). Cleaning solution (7×) came from ICN Biomedicals, Inc, while bovine serum albumin (BSA, fraction V, 99%) and α-D-glucose were purchased from Sigma. α-D-Glucose equilibrates with β-D-glucose in water. Borosilicate capillary tubes (5 μL, 388-μm i.d.) were obtained from VWR. Photoresist Microposit S 1813 and Microposit Developer were purchased from Shipley Co. (Marlborough, MA). Syringe needles came from Becton Dickinson & Co. (Franklin Lakes, NJ).

Preparation of Small Unilamellar Vesicles. SUVs formed from phospholipids, fluorescently labeled phospholipids, and biotinylated phospholipid mixtures were prepared using the Barenholz method.¹⁹ Briefly, lipids dissolved in chloroform were mixed together to the desired mole ratio. The solvent was evaporated in a stream of dry nitrogen followed by vacuum evaporation for an additional 4 h. The dried lipids were reconstituted in phosphate buffer (pH 7.4, ionic strength 150 mM) and sonicated with a titanium tip to form SUV solutions. The samples were centrifuged at 38 000 rpm (94500*g*) for 30 min, and then the supernatant was centrifuged again at 52 000 rpm (176900*g*) for 3 h using a Beckman ultracentrifuge L7 with a Ti-75 rotor.

Forming Phospholipid Bilayers inside Capillary Tubes. Borosilicate capillary tubes were cleaned in boiling surfactant (4:1 mixture of water and 7× cleaning solution) for 30 min. After extensive rinsing with water from a NANOpure Ultrapure water system (Barnstead, Dubuque, IA), they were baked in a kiln for 5 h at 400 °C and cut into 1-cm-length pieces using a glass cutter. DLPC SUVs, which contained 3 mol % NBD-PE as fluorescent tags, were made to flow through the capillary tubes where they fused to the surface to form single planar supported membranes. Excess vesicles were washed out with fresh PBS buffer (pH 7.4). The fluidity of the supported phospholipid bilayers inside the microcapillary tubes was confirmed by fluorescence recovery after photobleaching (FRAP)^{20,21} using an upright epifluorescence

- (16) Darst, S. A.; Ahlers, M.; Meller, P. H.; Kubalek, E. W.; Blankenburg, R.; Ribi, H. O.; Ringsdorf, H.; Kornberg, R. D. *Biophys. J.* **1991**, *59*, 387–396.
- (17) Herron, J. N.; Muller, W.; Paudler, M.; Riegler, H.; Ringsdorf, H.; Suci, P. A. *Langmuir* **1992**, *8*, 1413–1416.
- (18) Edmiston, P. L.; Saavedra, S. S. *J. Am. Chem. Soc.* **1998**, *120*, 1665–1671.

- (19) Barenholz, Y.; Gibbes, D.; Litman, B.; Goll, J.; Thompson, T.; Carlson, F. *Biochemistry* **1977**, *16*, 2806–2810.
- (20) Axelrod, D.; Koppel, D. E.; Schlessinger, J.; Elson, E.; Webb, W. W. *Biophys. J.* **1976**, *16*, 1055–1069.

microscope (E800, Nikon) equipped with a 1024 Micromax CCD camera. Images were captured with Metamorph software from Universal Imaging Corp.

Forming Phospholipid Bilayers inside Poly(dimethylsiloxane) Microchannels. The formation of phospholipid bilayer-coated microchannels has been described elsewhere.¹² Briefly, channels were formed by placing lithographically patterned poly-(dimethylsiloxane) (PDMS) molds (Dow Corning Sylgard Silicone Elastomer-184, Krayden, Inc.) into conformal contact with planar borosilicate coverslips. The molds were made by curing the low molecular weight polymer with a cross-linker on a photolithographically patterned master prepared by exposing and developing a photoresist patterned surface. The elastomeric mold, which bore the negative pattern of the master, was carefully peeled off and washed repeatedly with acetone and ethanol. Before contact was made with the glass substrate, the PDMS surface was rendered hydrophilic by oxygen plasma treatment for 15 s (PDC-32G plasma cleaner, Harrick Scientific, Ossining, NY). Glass coverslips, which served as floors for the microchannels, were cleaned in hot surfactant solution (ICN $\times 7$ detergent, Costa Mesa, CA), rinsed at least 20 times in purified water from the NANOpure Ultrapure Water System and then baked in a kiln at 400 °C for 4 h before use. A Harvard PHD 2000 syringe pump (Harvard Apparatus, Holliston, MA) was employed to infuse all solutions into the PDMS microchannels. Supported bilayer formation and quality inside the channels was confirmed by FRAP and quantitative fluorescence.

RESULTS AND DISCUSSION

Immobilization and Characterization of Phosphatase Catalyst in Microcapillary Tubes. Vesicles containing 0.1 mol % biotinylated lipids were fused to the microcapillary walls as described above in the Experimental Section. A solution of 5 mg/mL BSA in PBS buffer (pH 3.8) was injected and incubated for at least 1 h. This ensured that defect sites in the bilayer would be passivated before enzyme introduction. The BSA solution was washed out using a pH 9.8 buffer ($\text{Na}_2\text{CO}_3/\text{NaHCO}_3$, ionic strength 150 mM). The tube was incubated in the buffer overnight, as waiting several hours allowed BSA to fully reorganize at the interface. At this point, a solution of streptavidin-conjugated alkaline phosphatase (0.02 mg/mL) was made to flow into the tubes, incubated for 15 min, and washed out with the same pH 9.8 buffer. This relatively high protein concentration was employed to quickly saturate the surface biotin binding sites, and the pH of the washing buffer was chosen for maximum catalytic activity. In the next step, 0.136 mM 4-methylumbelliferyl phosphate in pH 9.8 buffer was added to an enzyme-coated capillary tube. The tube was placed under a fluorescence microscope, and the rate of product formation (7-hydroxy-4-methylcoumarin) was monitored by following the change in blue fluorescence intensity as a function of time (Figure 2, \circ). The same reaction then was repeated with several different concentrations of biotinylated lipids in the membrane (Figure 2). As can be clearly seen from the data, the observed reaction rate increased as the biotin concentration was raised from 0.1 to 1 mol % and leveled off at this value for higher concentrations. It should be noted that even the 0.0 mol % bilayer gave a small residual response, which was probably due to a tiny amount of enzyme nonspecifically adsorbed to the underlying substrate.

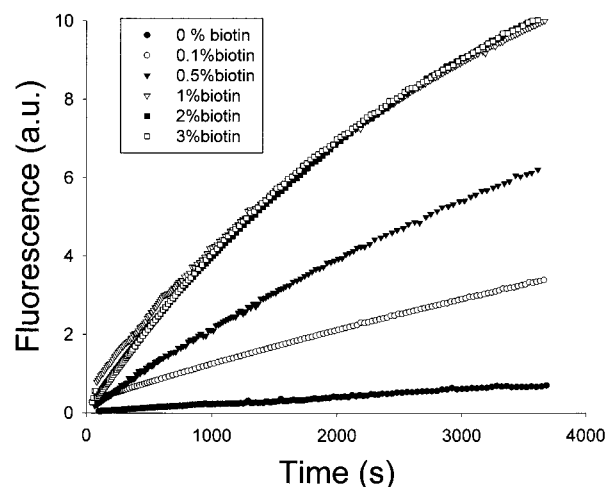


Figure 2. Fluorescence from the production of 7-methoxy-4-methylcoumarin versus reaction time from phosphatase enzymes immobilized on lipid bilayers containing various amounts of biotin. Each reaction was performed with an initial concentration of 0.136 mM 4-methylumbelliferyl phosphate.

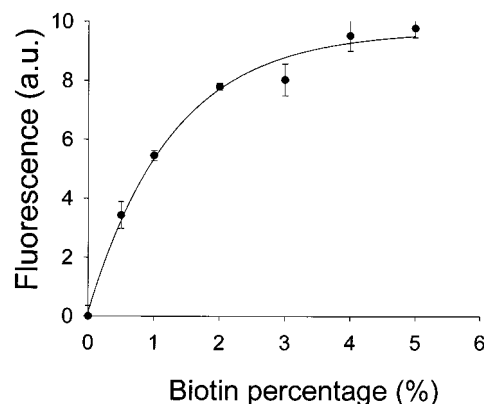


Figure 3. Fluorescence intensity from Texas Red-labeled streptavidin bound to DLPC supported bilayers as a function of biotin concentration in the bilayers. The initial concentration of streptavidin in the bulk solution was 0.01 mg/mL.

It is necessary to estimate the total enzyme concentration, $[E]_T$, inside the microcapillary tubes in order to find the absolute turnover rate of the catalyst. An approximate measure can be obtained by comparing the relative footprint sizes of streptavidin-conjugated phosphatase to streptavidin alone, since the size of the latter is well known. To achieve this, binding experiments of fluorescently labeled streptavidin were performed as a function of the mole percent of biotin in the membrane. The results are plotted in Figure 3. As can be seen from the data, the maximum amount of streptavidin that could be bound to the surface continued to rise with increasing biotin concentration until ~ 4 mol % and then saturated. This indicated that phosphatase-linked streptavidin occupied ~ 4 times greater surface area per molecule than streptavidin alone. Such a result is in line with expectations, as streptavidin has a molecular weight of 60 000, while the phosphatase (alone) is ~ 140 000 and the conjugate is 200 000. Two-dimensionally crystalline streptavidin has a $5.8 \text{ nm} \times 5.8 \text{ nm}$ unit cell.²² The footprint of crystalline streptavidin (33.6 nm^2) therefore provides a lower bound for streptavidin-linked phosphatase of ~ 4 times this value, 134 nm^2 .

(21) Soumpasis, D. M. *Biophys. J.* **1983**, *41*, 95–97.

(22) Kim, E. E.; Wyckoff, H. W. *J. Mol. Biol.* **1991**, *218*, 449–464.

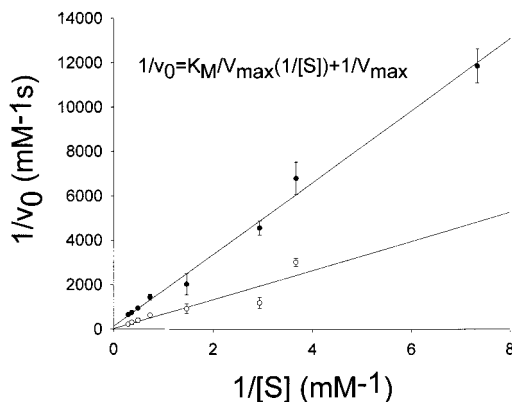


Figure 4. Lineweaver–Burk plots of the reciprocal initial reaction rates, $1/v_0$, versus the reciprocal of substrate concentration, $1/[S]$, for soluble, \circ , and immobilized, \bullet , streptavidin-conjugated alkaline phosphatase.

To obtain quantitative information on the turnover rate of the bilayer-supported enzyme, the initial reaction rate, v_0 , was measured as a function of substrate concentration, $[S]$. v_0 was determined by finding the slope (extrapolated to the origin) during the initial stage (first 300 s) for the change in fluorescence intensity versus time at each concentration tested. These data were plotted using the Lineweaver–Burk equation:²³

$$1/v_0 = (K_M/V_{\max})/[S] + 1/V_{\max}$$

where K_M is the Michaelis constant and V_{\max} is the velocity of the reaction when the active sites of the enzyme are saturated with substrate. A series of substrate concentrations ranging from 0.273 to 3.41 mM were made to flow into capillary tubes containing streptavidin-linked phosphatase on a 3 mol % biotinylated membrane (Figure 4, \bullet). The results revealed that $V_{\max} = 7.7 \pm 1.2 \mu\text{M/s}$ and $K_M = 12.5 \pm 2.9 \text{ mM}$. To calculate the turnover number, k_{cat} , for this reaction, it was necessary to obtain a reasonable estimate of $[E]_T$, as the turnover number is calculated from $k_{\text{cat}} = V_{\max}/[E]_T$. The surface area inside the capillary tube was $1.22 \times 10^{13} \text{ nm}^2$, so $\sim 1.5 \times 10^{-13} \text{ mol}$ of the enzyme could adsorb inside, using the footprint size obtained above. Because the volume of each capillary tube was $1.2 \times 10^{-6} \text{ L}$, the effective total enzyme concentration was $1.3 \times 10^{-7} \text{ M}$, leading to a turnover number, $k_{\text{cat}} = 60.6 \pm 9.4 \text{ s}^{-1}$.

The turnover number for the immobilized enzymes needs to be compared to enzymes in solution to determine what fraction of activity was maintained on the surface. The bulk solution value was measured using the same Lineweaver–Burk analysis with a streptavidin–phosphatase concentration of 0.02 mg/mL ($1 \times 10^{-7} \text{ M}$) and substrate concentrations ranging from 0.136 to 2.73 mM. The data are plotted as open circles (\circ) in Figure 4. In this case, $V_{\max} = 36.5 \pm 6.9 \mu\text{M/s}$ and $K_M = 14.0 \pm 2.7 \text{ mM}$. The turnover number in bulk solution was $k_{\text{cat}} = 365 \pm 69 \text{ s}^{-1}$.

From the calculations above, the turnover rate in solution was roughly a factor of 6 greater than the surface-bound enzyme. There are probably several factors contributing to the apparent difference in reaction rate between the immobilized and soluble

enzymes. The first stems from the obstruction of active sites at the interface. Steric effects have often been observed for immobilized proteins when their binding pockets face toward the surface.²⁴ As shown in Figure 1, the alkaline phosphatase used here had two active sites for dephosphorylation. Depending upon the packing density and protein orientation, some of these may not have been available for reaction. Furthermore, since the streptavidin-conjugated alkaline phosphatase was prepared by generic chemical cross-linking, the active sites on even neighboring alkaline phosphatases may have had different orientations relative to the underlying streptavidin. If these steric effects strongly blocked the substrate from getting to the most buried locations, this could have caused a significant reduction in turnover rate.

Another reason for the apparent difference in turnover between the immobilized enzymes and those in solution probably stemmed from an overestimation of enzyme number density at the surface, leading to an underestimation of k_{cat} in the immobilized case. Two important factors could have contributed to this. First, the footprint size of the streptavidin-conjugated phosphatase was almost certainly underestimated because of the use of crystalline streptavidin dimensions. Furthermore, our calculations assumed 100% enzyme coverage on the inside of the microcapillary tubes. This was not completely accurate as BSA rather than the supported lipid bilayers covered some portions of the surface. It therefore should be stated that the factor of 6 difference in turnover rate represented an upper bound to the difference. Finally, any portion of the bound enzyme that was denatured by this interface would, of course, have led to a decrease in the measured turnover rate.

Immobilization and Characterization of Phosphatase Catalyst in Microchannels: One-Shot Lineweaver–Burk Studies.

The next set of dephosphorylation reactions was carried out inside a parallel array of bilayer-coated PDMS microchannels (Figure 5). The apparatus was designed to simultaneously measure the reaction rates of 12 independent concentrations of substrate created by series dilution from the introduction of a single aliquot. Several methods for designing concentration diluters have already been shown for microfluidics.^{25–27} In our apparatus,²⁸ two streams of liquid were combined at a Y-junction and allowed to diffuse into each other as they flowed downstream side by side.²⁹ Such diffusional mixing was possible because the Reynolds number inside the channel was sufficiently low to prevent turbulence. After a fixed distance (2 cm), the main channel was partitioned into a series of smaller channels that emanated from the main flow stream. Substrate could be infused in one inlet port while pure buffer was injected into the other. This method created a dilution series that ranged over a factor of 33 in concentration from the first to the last microchannel. At the opposite end of the device, the channels were recombined into a common outlet. Inspired

(23) Voet, D.; Voet, J. G. *Biochemistry*, 2nd ed.; John Wiley and Sons: New York, 1995.

(24) Spinke, J.; Liley, M.; Guder, H. J.; Angermaier, L.; Knoll, W. *Langmuir* **1993**, *9*, 1821–1825.

(25) Jacobson, S. C.; McKnight, T. E.; Ramsey, J. M. *Anal. Chem.* **1999**, *71*, 4455–4459.

(26) Jeon, N. L.; Dertinger, K. W.; Chiu, D. T.; Choi, I. S.; Stroock, A. D.; Whitesides, G. M. *Langmuir* **2000**, *16*, A-F.

(27) Dertinger, S. K.; Chiu, D. T.; Jeon, N. L.; Whitesides, G. M. *Anal. Chem.* **2001**, *73*, 1240–1246.

(28) Holden, M. A.; Jung, S. Y.; Cremer, P. S., to be published.

(29) Weigl, B. H.; Yager, P. *Science* **1999**, *283*, 346–347.

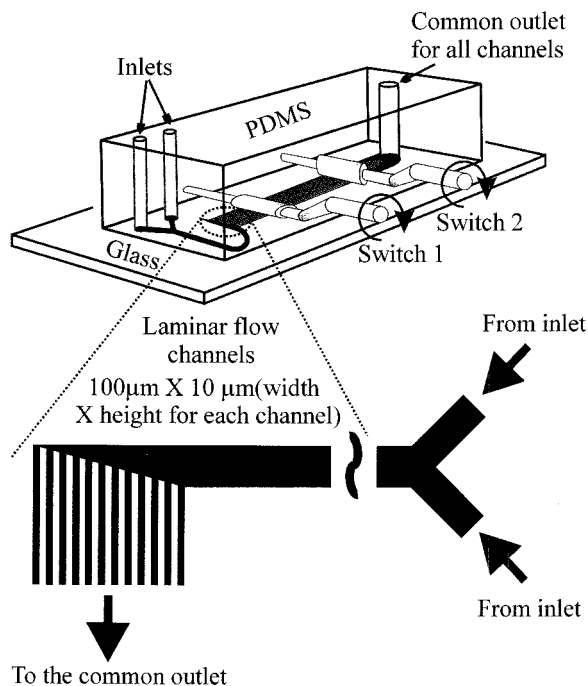


Figure 5. Schematic diagram of the apparatus used for a one-shot measurement of phosphatase activity. Twelve channels ($100\ \mu\text{m}$ wide \times $10\ \mu\text{m}$ high) spaced $50\ \mu\text{m}$ apart are connected to Y-shaped inlets through a $2\ \text{cm} \times 600\ \mu\text{m}$ (length \times width) mixing channel.

by the work of Unger and co-workers,³⁰ simple mechanically operated switches were designed by making elliptical holes in a plane $\sim 2\ \text{mm}$ above the 12-channel array and inserting elliptical metal needles whose shapes matched those of the holes. Turning the needles such that the wide axis was parallel to the array allowed liquid to flow inside the channels. Alternatively, when the needles were turned such that the wide axis was normal to the array, the top of the channels pressed against the floor causing complete shutoff of liquid flow.

The device was operated in the following manner. Small unilamellar DLPC vesicles containing 3 mol % biotinylated lipids flowed through the two inlet ports and fused to the walls and floor of the device to create a uniform supported bilayer coating. Excess vesicles were then washed out by flowing pure buffer. The channels were passivated with BSA in the same fashion as described above for the microcapillary tubes and incubated overnight. At this point, switch 1 (Figure 5) was closed and streptavidin-conjugated phosphatase ($0.2\ \text{mg/mL}$, pH 9.8) was added through the common outlet channel. Mixing occurred by continuously rotating switch 2 between the open and closed state for a period of 10 min. The switching process created a series of squeeze/release events, which efficiently mixed the protein solution into the channels. This procedure allowed the phosphatase to coat the microchannels between switch 1 and the common outlet, while leaving the front of the device protein free. After protein binding was completed, both switches were rotated to the open position and pure buffer was used to flow out excess enzyme. Following this, a solution of $3.41\ \text{mM}$ 4-methylumbelliferyl phosphate in pH 9.8 buffer was pumped through one inlet port while pure buffer was pumped through the other. After

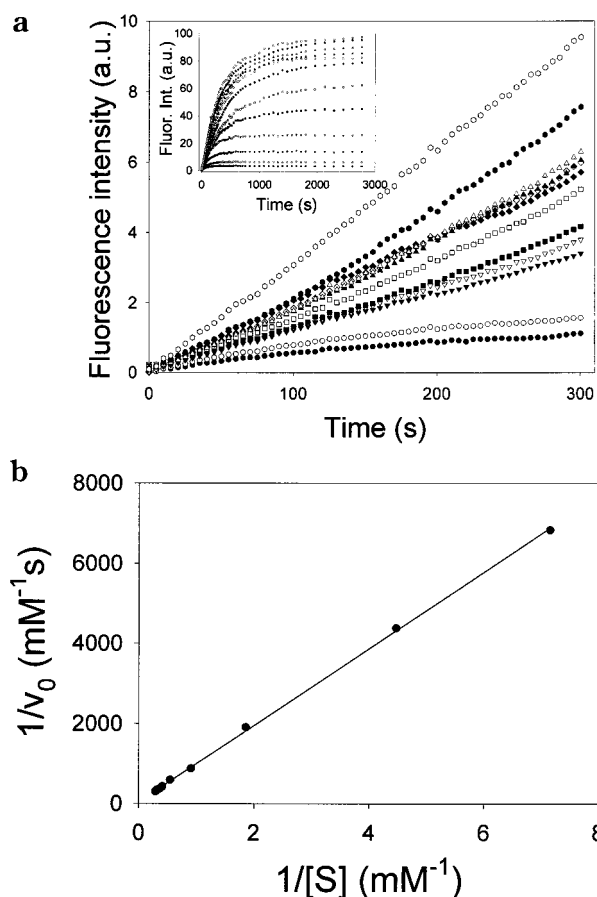


Figure 6. (a) Fluorescence intensity of 7-methoxy-4-methylcoumarin produced in the first 300 s of reaction by the phosphatase immobilized inside 12 channels: \bullet , 1; \circ , 2; \blacktriangledown , 3; ∇ , 4; \blacksquare , 5; \square , 6; \blacklozenge , 7; \lozenge , 8; \blacktriangle , 9; \triangle , 10; \bullet , 11; \circ , 12. The inset shows the same data set for the entire length of the experiment ($\sim 3000\ \text{s}$) (b) Lineweaver-Burk plot of the reciprocal of substrate concentrations for the immobilized streptavidin-conjugated phosphatase inside the arrayed microfluidic channels. The concentrations of 7-methoxy-4-methylcoumarin ranged from 0.103 to $3.41\ \text{mM}$.

allowing sufficient time to completely fill the channel array with substrate solution (several minutes), both switches were closed, the pump was turned off, and the fluorescence intensity of the product in all channels was followed simultaneously by epifluorescence microscopy. The rate of product formation as a function of time is plotted in Figure 6a.

The initial reaction rate (v_0) was obtained by measuring the slope of the change in fluorescence intensity versus time for each channel in Figure 6a for the first 300 s of the experiment as before. To determine the initial concentration of substrate in each channel, the total fluorescence intensity upon completion of the reaction (inset of Figure 6a) was compared to that of known product concentrations and it was assumed that the reaction went to completion in each case. Control experiments revealed that the fluorescence intensity was linearly related to the initial substrate concentration under these conditions. The data obtained from these measurements were then utilized to make a Lineweaver-Burk plot (Figure 6b). The results revealed that $k_{\text{cat}} = 51.1 \pm 3.2\ \text{s}^{-1}$ and $K_M = 16.2 \pm 1.3\ \text{mM}$, which were the same as the values obtained inside the microcapillary tubes within experimental error (Figure 4). This demonstrated that the combined PDMS-glass

(30) Unger, M. A.; Chou, H. P.; Thorsen, T.; Scherer, A.; Quake, S. R. *Science* **2000**, *288*, 113–116.

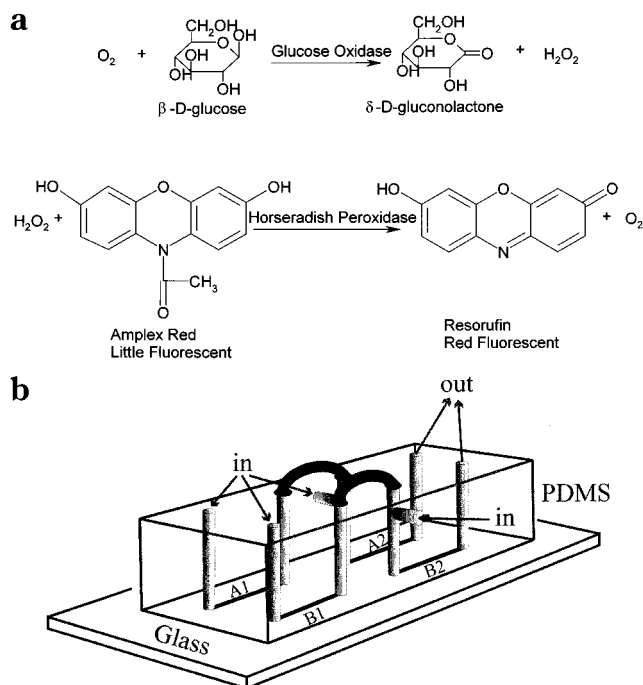


Figure 7. (a) Reaction scheme for the sequential reactions catalyzed by glucose oxidase and horseradish peroxidase. (b) Schematic representation of the microfluidic device used for the two-step glucose detection reaction.

surface was approximately as amenable for preserving enzyme activity upon immobilization as were the simpler microcapillary tubes. It should be further noted that the signal-to-noise ratio from the microchannel experiments was superior to that of the microcapillary tube data (Figures 4 and 6). Indeed, the error bars for this experiment were approximately the size of the filled circles used to plot the data. This was only about one-third the size of those from the microcapillary tube measurements. One important reason for the difference is the fact that all the data were collected simultaneously. Errors, therefore, associated with flicker in the Hg arc lamp in producing the fluorescent signal would be greatly reduced. Furthermore, taking all the data simultaneously took ~ 1 order of magnitude less time than preparing and measuring each stable concentration separately. The assay was stable enough that the product could be flowed out, new substrate introduced, and the experiment repeated. This was done up to 10 times over the course of 2 days without noticeable changes in the data obtained.

Exploiting Immobilized Enzymes inside Microchannels To Perform a Coupled Set of Chemical Reactions. The methods presented above for enzyme immobilization inside microfluidic channels affords the opportunity to run multistep chemical reactions within lab-on-a-chip devices. Substrates can be introduced over a first immobilized enzyme and the products may then continue downstream to additional sets of enzymes for further reactions. Indeed, it could be easily envisioned that complex multistep syntheses could be performed in this manner. To demonstrate this principle with the chemistry developed above, we chose a simple two-step process often exploited for the detection of glucose (Figure 7a). The process operates by employing glucose oxidase in a first step to oxidize β -D-glucose to δ -D-gluconolactone and hydrogen peroxide. The H_2O_2 is then used in a second step to convert Amplex Red, a molecule with little fluorescence, to the highly fluorescent product, resorufin.

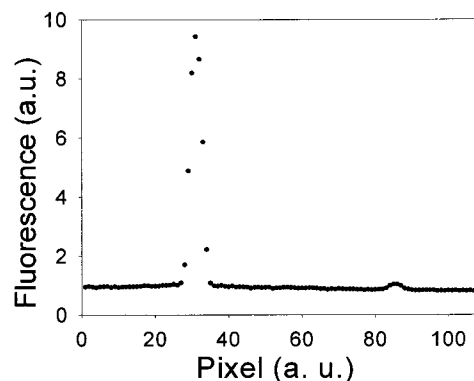


Figure 8. Line scan of resorufin fluorescence intensity across channels A2 and B2.

A schematic diagram of the microfluidic device used for the two-step reaction is shown in Figure 7b. It was capable of running two experiments simultaneously. On one side (A) the experiment was run in the presence of glucose and on the other (B) the chemistry was identical, but no glucose was used. Each microchannel was divided into two parts (A1 and A2, B1 and B2) and connected by a reversibly attachable U-shaped plastic tube (700 μm in diameter). With the tubes unattached, SUVs containing 3 mol % biotinylated lipids were fused to the channel surfaces throughout the device, excess SUVs were removed, and the whole device was passivated with BSA. After washing out the excess BSA with pH 7.4 PBS buffer, avidinD-conjugated glucose oxidase (0.5 mg/mL) was made to flow into A1 and B1, while streptavidin-conjugated horseradish peroxidase (0.2 mg/mL) was infused into A2 and B2. Both were incubated in their respective channels for 20 min in pH 7.4 PBS buffer solution and washed out for 40 min in pure buffer. At this point, the U-shaped tubes were attached.

To commence the reactions, freshly prepared β -D-glucose (10 mg/mL in PBS 7.4 buffer, pregassed with oxygen) was infused into the inlet of A1 while pure buffer was infused into B1. Amplex Red (1 mM in DMSO/ H_2O = 1/10) flowed in via branched sidearms of A2 and B2 where it met up with any products of A1 and B1 and flowed together into A2 and B2. The red fluorescent signal of the resorufin product was monitored by fluorescence microscopy. The line scan of the fluorescence across the channels is shown in Figure 8. The results indicated that the fluorescence intensity from the control channel (B) was $\sim 2\%$ of that from experimental channel. This residual intensity in the control channel was due to the fact that Amplex Red itself is weakly fluorescent. The entire experiment was repeated by introducing both the Amplex Red and glucose through A1 and Amplex Red through B1. The results were identical. This procedure clearly demonstrated the utility of employing immobilized enzymes in microfluidic channels for carrying out multistep chemical reactions.

CONCLUSION

In the experiments presented here, enzymes were immobilized in phospholipid bilayer-coated microcapillary tubes and microfluidic channels. The turnover numbers for phosphatase immobilized inside microcapillary tubes and microfluidic channels were similar and represented a reasonable fraction of the corresponding bulk value. A one-shot Lineweaver–Burk plot using

arrayed microfluidic channels demonstrated the feasibility of using microchannels to obtain kinetic data rapidly with a high S/N ratio. Serial enzyme reactions inside a microfluidic device were established to show the potential application of this general methodology to multistep chemical synthesis.

ACKNOWLEDGMENT

This work was supported by ARO (DAAD19-01-1-0346), an ONR-YIP Award (N00014-00-1-0664), the Texas Advanced Tech-

nology Program (Grant 010366-0181-1999), startup monies from Texas A&M University, a Nontenured Faculty Award from 3M Corp., and a Research Innovation Award from the Research Corporation of America (RI0437).

Received for review July 20, 2001. Accepted October 10, 2001.

AC010822U